frontiers | Frontiers in Earth Science

ORIGINAL RESEARCH
published: 20 May 2022
doi: 10.3389/feart.2022.882058

Causes of Tunnel Diseases in a Karst Stratum and Remediation Measures: A Case Study

Shen Jiajia[1], *Zhang Hu*[2], *Wan Li*[1], *Zhang Changan*[1]*, *Shao Xing*[1], *Lin Zanquan*[2] and *Song Jie*[1]*

[1]Shandong Provincial Communications Planning and Design Institute Group Co., Ltd., Jinan, China, [2]School of Civil Engineering, Central South University, Changsha, China

Highway tunnels operated in karst areas are prone to serious structural diseases such as water–mud inrush, lining tension and cracks, and road humps. This article reviews the historical diseases of the tunnel based on the Nanshibi Tunnel project. The cause analysis of the structural diseases of Nanshibi Tunnel was performed on the basis of a refined geophysical prospecting scheme for the complex karst geological structure environment. A series of comprehensive treatments were conducted to address the tunnel diseases in the karst area. The treatments included surrounding rock grouting, lining replacement, and adding inverted arches. The results show that the refined geophysical prospecting scheme and disease remediation idea for the complex karst geological structure environment proposed herein can realize the full coverage and accurate detection of karst structures, water passage, and tunnel-lining diseases. The proposed scheme can effectively solve the technical problems of karst tunnel diseases that occur repeatedly and are difficult to be completely rectified. Finally, specific engineering practice suggestions were proposed for tunnel disease remediation in the karst area.

Keywords: karst tunnel, structural diseases, comprehensive detection, disposal measures, numerical calculation

OPEN ACCESS

Edited by:
Dongxing Wang,
Wuhan University, China

Reviewed by:
Jun Yu,
Nantong University, China
Zhang Cong,
Central South University of Forestry and Technology, China

***Correspondence:**
Zhang Changan
sdjxzca@163.com
Song Jie
sjysongjiejack@163.com

Specialty section:
This article was submitted to Geohazards and Georisks, a section of the journal Frontiers in Earth Science

Received: *23 February 2022*
Accepted: *29 March 2022*
Published: *20 May 2022*

Citation:
Jiajia S, Hu Z, Li W, Changan Z, Xing S, Zanquan L and Jie S (2022) Causes of Tunnel Diseases in a Karst Stratum and Remediation Measures: A Case Study. Front. Earth Sci. 10:882058. doi: 10.3389/feart.2022.882058

INTRODUCTION

Limestone is one of the most widely distributed minerals in the Earth's crust. Large amounts of limestone are distributed in Northeast China, North China, East China, Southwest China, Central South China, and Tibet. The main component of limestone is calcium carbonate, which causes corrosion and crystallization under the action of groundwater, especially flowing water. Therefore, limestone strata in water-rich areas usually form many water channels under erosion by water flow, resulting in the formation of karst phenomena topography with features such as karst troughs and caves, underground rivers, karst halls, and other structures. With the vigorous development of China's transportation industry (Ding et al., 2017; Gong et al., 2017; Gong et al., 2019), numerous tunnels have been built in the limestone strata (He and Wang, 2013). Because of the hydrogeological conditions in karst areas, tunnels often suffer from water–mud inrush, collapse, and lining cracking during construction and operation (Gongyu and Wanfang, 1999; Huang et al., 2020; Liu et al., 2020; Jia et al., 2021). These problems directly affect the regular use and durability of the tunnel structure and even traffic and structural safety in serious cases (Lei et al., 2020; Lei et al., 2021a).

As yet, in-depth research has been conducted on the disease assessment and prediction of tunnel engineering in karst areas (Zhu and Li, 2020; Lei et al., 2021b; Junfeng et al., 2021; Tang

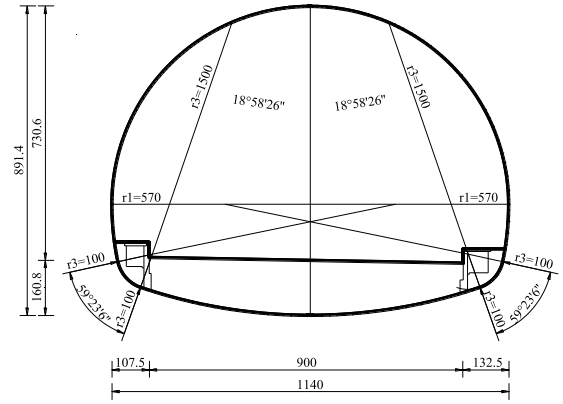

FIGURE 1 | Tunnel contour map (unit: cm).

et al., 2021), disease-formation mechanism (Huang et al., 2017; Rui, 2019; Wang et al., 2019), construction control technology (Min-qing et al., 2007; Yao et al., 2017; Lei et al., 2021c; Zhao et al., 2021), disease remediation measures (Richards, 1998; Fan et al., 2018; Bangning, 2021), etc., and good research achievements have been obtained. However, many engineering practices show that the present conventional disease treatment methods applied to active karst tunnels are often incomplete treatments conducted at one time and the problems are likely to recur at a later stage. For example, the safety of the Nanshibi Tunnel structure is endangered by many major diseases, such as lining cracking, water and mud inrush, and inverted arch uplift. These problems have not been solved even after repeated treatments. The scale of the disease, number of dangerous situations, and frequency of treatment are rare in China and other countries.

DESIGN AND DISEASE SITUATION OF NANSHIBI TUNNEL

Design Condition

Nanshibi Tunnel is a separate tunnel. The starting and ending pile numbers of the left line are ZK172 + 136 and ZK173 + 060, respectively, extending to a length of 924 m. The starting and ending pile numbers of the right line are YK172 + 136 and YK173 + 100, respectively, extending to a length of 964 m. The maximum buried depth of the tunnel is about 110 m. The clear width of the tunnel construction boundary is 10.75 m, and the clear height is 5.0 m. The width of the carriageway (including the margin verge) is 9.0 m, and the left and right widths of the maintenance road are 0.75 and 1.0 m, respectively, as shown in **Figure 1**.

The tunnel area is a dissolution landform with structural denudation and erosion, and it crosses the Jinhe River and Yuanhe River systems. A reservoir is present on the north side of the tunnel. The main adverse geological feature in the tunnel site area is the karst topography, and a large number of stone teeth, karst grooves, and caves are exposed on the surface, which is a typical karst water-rich area. In addition, the tunnel is located in the Pingxiang–Xinjian fault zone, where secondary faults are developed, and the rock mass is crushed by intense extrusion or cutting, with poor stability, as shown in **Figure 2**.

Diseases Over the Years

Structural diseases such as lining cracking, water leakage, and inverted arch uplift have occurred in the Nanshibi Tunnel since its opening in 2008. Even after treatment and maintenance, a large number of diseases occurred successively from 2010 to 2017, as shown in **Figures 3**, **4**.

(1) On 23 May 2008, local seepage was found during the acceptance of the main subgrade project of Nanshibi Tunnel. Very wide concrete cracks were seen in the interval ZK172 + 470 to +494, and the inverted arch was locally uplifted to 12 cm and accompanied by seepage containing limestone sediment and other substances.
(2) Since 6 May 2010, this area received a large amount of rain continuously, and many karst collapses occurred on the surface. The secondary lining of the tunnel cracked, and the road surface was uplifted. Water gushing and mud inrush occurred at ZK172 + 464 to ZK172 + 520 and at ZK172 + 630 and YK172 + 627. Karst collapse and falling caves developed on the top of the cave.
(3) In the first half of 2012, the precipitation was considerable, and the groundwater level increased. Because of the heavy rainfall, the road surface in the tunnel section YK172 + 210 to YK172 + 650 became moist and watery. Local pavement cracks and pits formed, and water seeped from the cracks and pits.
(4) During heavy rain on 24 May 2014, many instances of water bursts occurred at the left arch foot of ZK172 + 300 of the tunnel, and the water column was sprayed onto the carriageway. The diameter of the water column was about 10 cm, and the water was turbid milky white with a small amount of sand. Mountain collapse occurred at the top of the cave treated with block stones and cement concrete, with a total area of about 30 m^2. The soil near the collapse cracked, and the crack width is about 30 cm.
(5) Heavy rainfall occurred on the afternoon of 15 May 2015. Water and mud inrush occurred at the ZK172 + 520 section of the tunnel at noon on May 16, and sediment gushed from the cover plate of the left drainage ditch. The sediment covered the whole pavement, which was 26 m long and 8–10 cm thick with an area of about 200 m^2. The left maintenance road was tilted, and the maximum tilt height difference was 20 cm.
(6) Eight days of continuous rainfall occurred in May 2016. On 9 May, serious water leakage occurred at the construction joint of the YK172 + 600 section of the tunnel, forming a water curtain hole. Two pavement core holes showed significant inrush of water. Collapse pits with a diameter of 6 m and a depth of 3 m appeared on the tunnel roof.

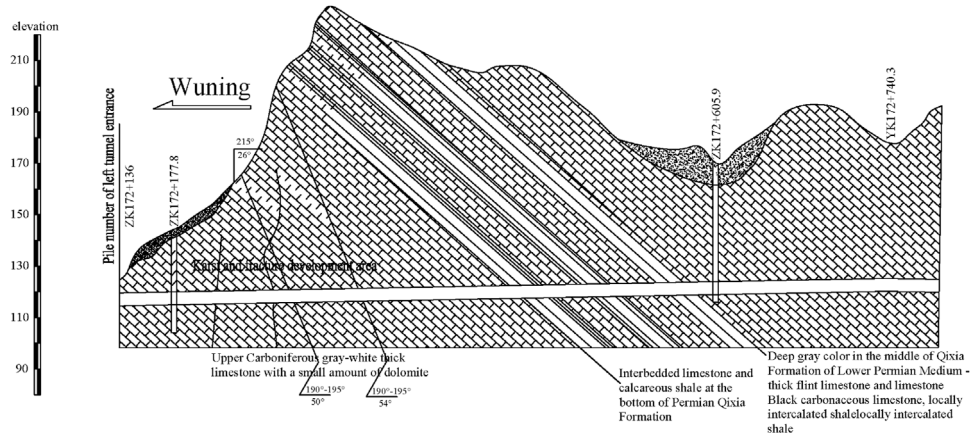

FIGURE 2 | Longitudinal section of Nanshibi Tunnel.

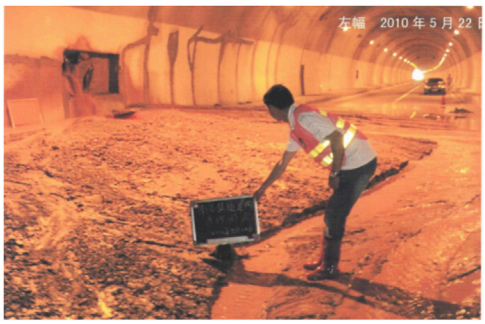

FIGURE 3 | Water–mud inrush in the tunnel.

FIGURE 4 | Cracking of the tunnel lining.

CAUSE ANALYSIS OF DISEASES IN NANSHIBI TUNNEL

To accurately identify the causes of diseases and the current structural stability of Nanshibi Tunnel, a detailed investigation of geological and structural diseases was performed by using various geophysical methods to calculate and analyze the stability of the tunnel structure.

Refined Exploration of Karst Structures

To ensure exploration accuracy, various geophysical methods are fully used in exploration. Examples of such methods are the high-density resistivity method, transient electromagnetic method, geological radar method, and seismic imaging method. These methods are used to complement and verify each other to realize the comprehensive exploration of tunnel disease, karst structure, and water passage. The exploration of the surrounding rocks proceeds gradually from region to detail, and its basic scheme is shown in **Figure 5**.

A comprehensive analysis of the geophysical prospecting results (e.g., the typical results shown in **Figures 6**, **7**) reveals the following about the karst and water-diversion channel of Nanshibi Tunnel:

(1) The surrounding rock of the ZK172 + 438 to ZK172 + 657 section of the left tunnel and YK172 + 345 to YK172 + 570 section of the right tunnel is relatively broken, with developed karst fissures. The local rock mass is broken and water-rich, and the karst caves are concentrated in this area. The spatial distribution of the fracture zone, tunnel sidewall, and vault-fractured area is generally irregular.
(2) The areas with relatively concentrated karst development are located in the YK172 + 468 to YK172 + 536 and YK172 + 590 to YK172 + 657 sections. Several karsts intersect with the left and right lines of the tunnel and gradually develop from the left to the right line of the tunnel to the lower depth.
(3) Analysis of the water content of the fracture zone showed that the water content of the tunnel floor is higher than that of the sidewall, and the water content of the floor of the right tunnel is higher than that of the left tunnel. The water-bearing area of the surrounding rocks of the floor is less than 4 m from the road surface.

Bearing Capacity of the Tunnel Lining

The surrounding rock grade of Nanshibi Tunnel is IV–III. The main types of secondary lining are S4, S4-1, and S3. The S4-1 lining has water leakage disease, while S4 and S3 linings exhibit

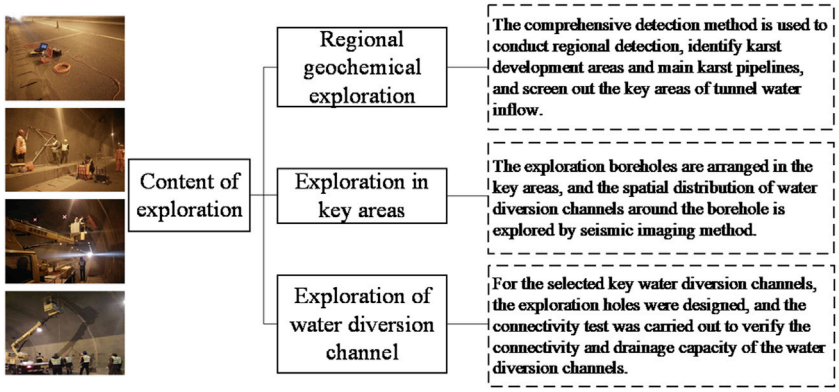

FIGURE 5 | Exploration scheme of the surrounding rock of the tunnel.

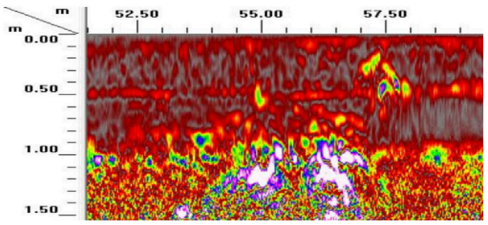

FIGURE 6 | Water-diversion channel under an inverted arch in ZK172 + 592 to 595 sections.

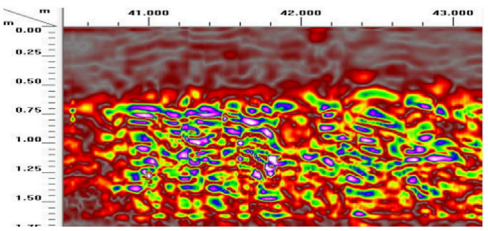

FIGURE 7 | Water-diversion channel behind the right wall of ZK172 + 607 to 609 sections.

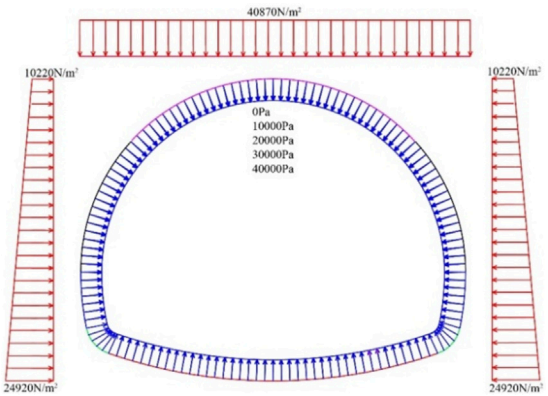

FIGURE 8 | Load structure model with an inverted lining section (S4-1 and S4).

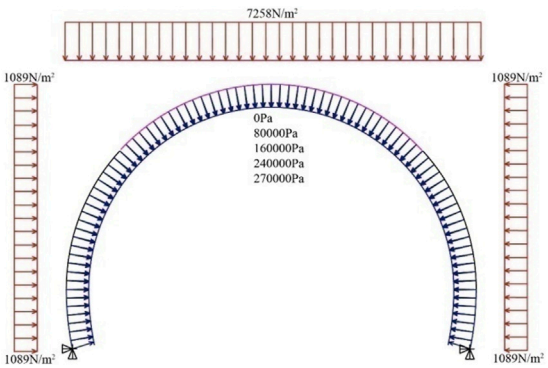

FIGURE 9 | Load structure model without an inverted lining section (S3).

water leakage disease and insufficient lining thickness. Accordingly, the load structure method was adopted to establish the calculation model of the typical lining in disease areas under hydrostatic pressure. The calculation models of the load structure are shown in **Figures 8**, **9**. The calculation parameters are listed in **Tables 1**, **2**.

The internal force calculation results of the typical secondary lining of the tunnel are shown in **Figures 10**, **11**. The results are as follows:

(1) The internal force distributions of the inverted arch lining (S4-1 and S4) and noninverted arch lining (S3) are different because of the differences in the structural form and constraint conditions. In general, because of the closed structure of the ring, the internal force distribution of the lining with the inverted arch is more even, and the force performance is more superior. The most unfavorable lining position with the inverted arch is mainly distributed in the vault, arch shoulder, and arch foot, whereas the most

TABLE 1 | Lining calculation parameters.

Lining type	Elastic modulus e (kpa)	Volume weight γ (kn/m^3)	Area a (m^2)	Inertial moment i (m^4)
S4-1	2.95e7	25	0.40	0.0053
S4	2.95e7	23	0.40	0.0053
S3	2.95e7	23	0.35	0.0035

TABLE 2 | Parameters of the surrounding rock.

Surrounding rock grade	Volume weight Γ (kn/m^3)	Internal friction angle (°)	Poisson's ratio	Stratum spring (mpa/m)
Grade IV	22.00	55.00	0.325	450
Grade III	24.00	65.00	0.275	850

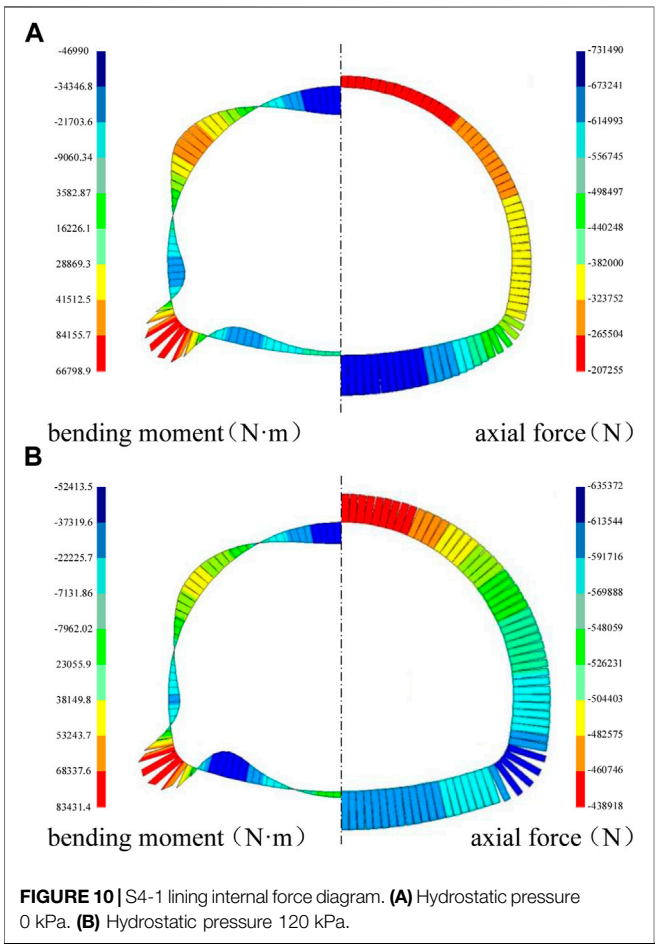

FIGURE 10 | S4-1 lining internal force diagram. **(A)** Hydrostatic pressure 0 kPa. **(B)** Hydrostatic pressure 120 kPa.

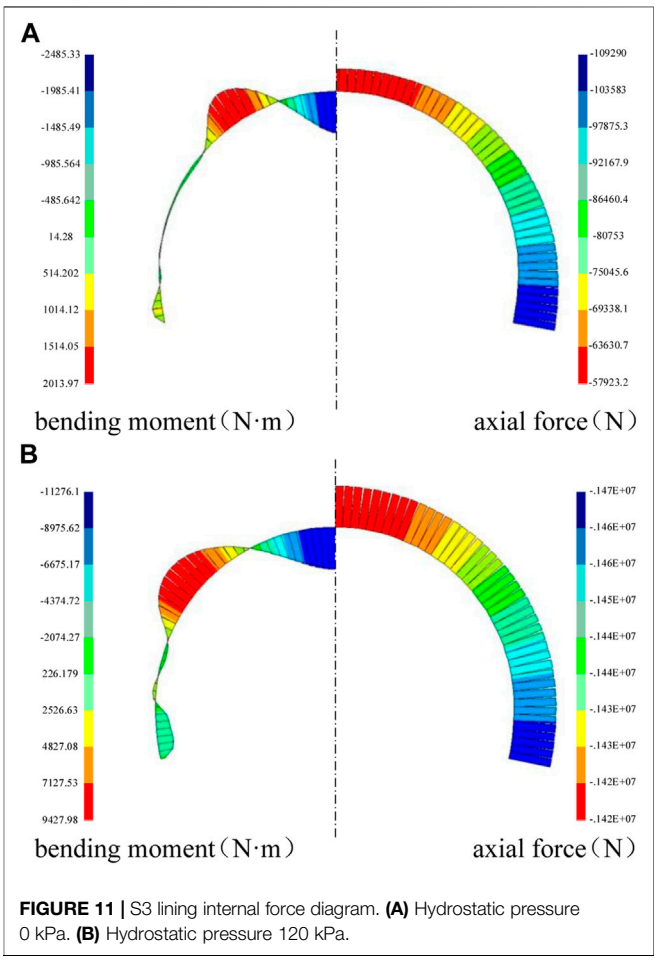

FIGURE 11 | S3 lining internal force diagram. **(A)** Hydrostatic pressure 0 kPa. **(B)** Hydrostatic pressure 120 kPa.

unfavorable position of the lining without the inverted arch is the vault and arch shoulder.

(2) With the gradual application of hydrostatic pressure, the internal force of the secondary lining of the tunnel also changes. For the lining with an inverted arch, the structural bending moment and axial force of the arch wall and vault increase gradually and the axial force of the inverted arch decreases gradually. The bending moment and axial force of the whole section increase gradually for the lining without an inverted arch. Therefore, the effect of hydrostatic pressure increases the internal force of the structure, causing adverse effects. The adverse effect is remarkable, especially for the inverted arch when the bending moment increases as the axial force decreases.

TABLE 3 | Secondary lining safety factor.

Pile number	Lining type	Lining structure	Design thickness (cm)	Gaged thickness	Hydrostatic pressure (kPa)	Factor of safety	Regularization coefficient
ZK172 + 482	S4-1	Reinforced concrete	40	40–42 cm	0	3.41	2.0
					120	1.22	2.0
ZK172 + 514	S4	Plain concrete	40	36–37 cm	0	3.73	3.6
					112	0.91	3.6
ZK172 + 588				22–39 cm	0	3.32	3.6
					100	1.17	3.6
ZK172 + 600	S3	Plain concrete	35	26–33 cm	0	13.55	3.6
					92	6.71	3.6

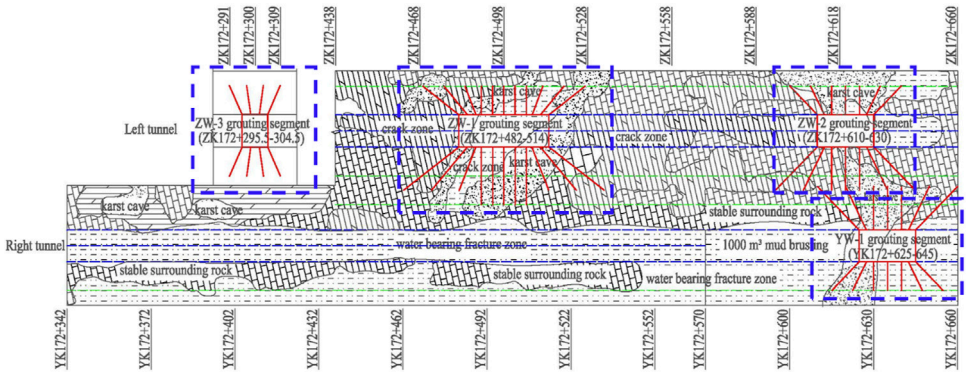

FIGURE 12 | Plane layout of the curtain grouting of the surrounding rock.

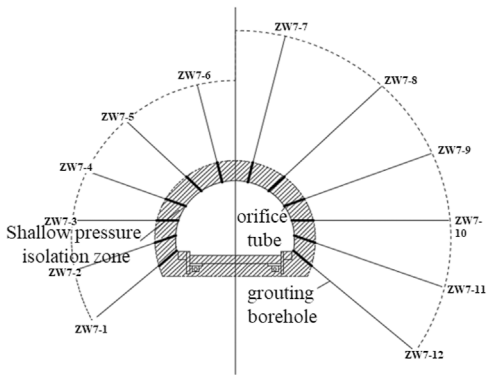

FIGURE 13 | Schematic diagram of the curtain grouting of the surrounding rock.

(3) According to the "Design Specification for Traffic Engineering of Highway Tunnel" (JTG D71-2004-2004, 2004), the secondary lining structure is checked according to the principle of the damage stage method, and the results are listed in **Table 3**. The calculation results show that the safety factors of all sections, except those of the ZK172 + 588 section, can meet the specification requirements without hydrostatic pressure. Because the actual lining thickness of the ZK172 + 588 section is lower than the design thickness and the bearing capacity of the section is greatly weakened, the safety factor still did not meet the requirements of the specification without hydrostatic pressure. When the lining section is subjected to hydrostatic pressure, the safety factor of the structure decreases sharply. The safety factors of the calculated sections, except those of the ZK172 + 600 section, do not meet the specification requirements. In particular, the safety factor of ZK172 + 514 is 0.91 < 1.0, and the most unfavorable part of the section is likely to fail or get damaged, endangering tunnel safety.

Cause Analysis

Based on the aforementioned investigation and calculation results, the causes of diseases in Nanshibi Tunnel can be determined.

(1) The tunnel has a karst structure with many water-diversion channels. In the rainy season, a large amount of precipitation infiltrates into the mountains, resulting in a rapid increase in the groundwater head and hydrostatic pressure on the tunnel structure. When the combined effect of the surrounding rock load and hydrostatic pressure exceeds the bearing capacity of the local weak points of the secondary lining structure of the tunnel or the impermeability of construction joints and settlement joints, diseases such as lining cracking, breakdown, and water–mud inrush occur.

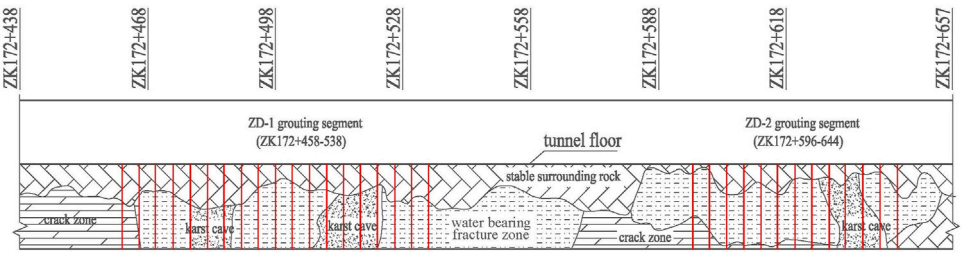

FIGURE 14 | Grouting layout of the left line of the tunnel.

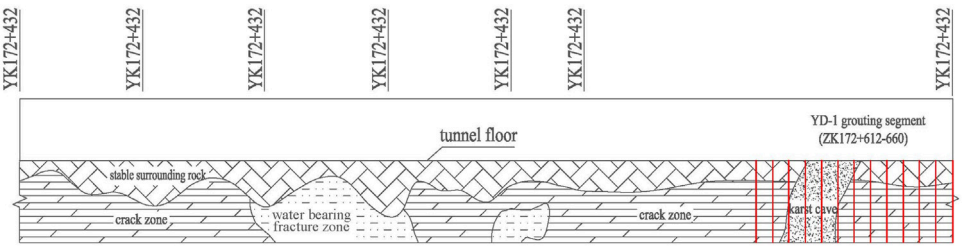

FIGURE 15 | Grouting layout of the right line of the tunnel.

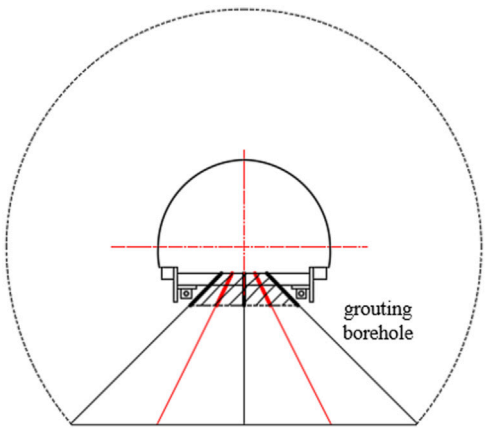

FIGURE 16 | Schematic diagram of the cross section of the tunnel floor grouting.

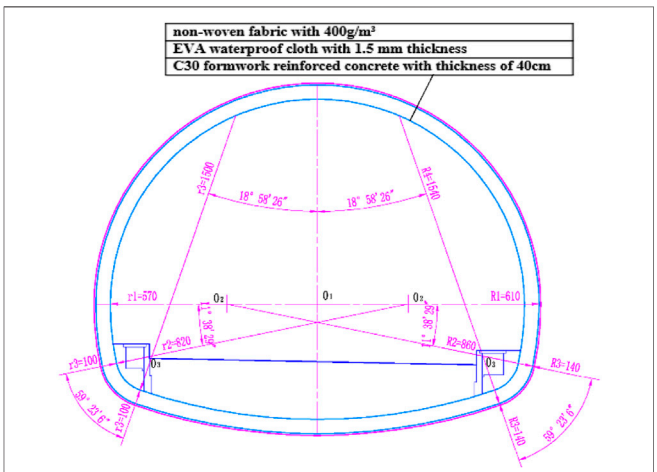

FIGURE 17 | Cross section of the replacement tunnel lining (unit: cm).

(2) The water-diversion channels also developed in the local tunnel without an inverted arch. Because of the absence of an inverted arch lining constraint, the hydrostatic pressure directly acts on the tunnel pavement base. When the pavement weight is insufficient to resist the hydrostatic pressure below, problems such as pavement uplift, water gushing, and cable trench tilt occur.

(3) Part of the treatment scheme only considered drainage without considering plugging for leakage water. When the amount of groundwater is excessive, the water head cannot be reduced in time, and the pressure on the tunnel lining structure is enormous.

(4) Although some treatment schemes consider plugging the cracks in the surrounding rock, the hydrostatic pressure of the surrounding rock at the location of the disease treatment during the rainy season is not effectively reduced because of the incomplete discovery and sealing of the water-diversion channel. Hence, enormous pressure is still imposed on the tunnel lining structure.

(5) The reinforcement strength of the secondary lining at the diseased location of the tunnel is insufficient to resist the combined effect of the surrounding rock pressure and high hydrostatic pressure.

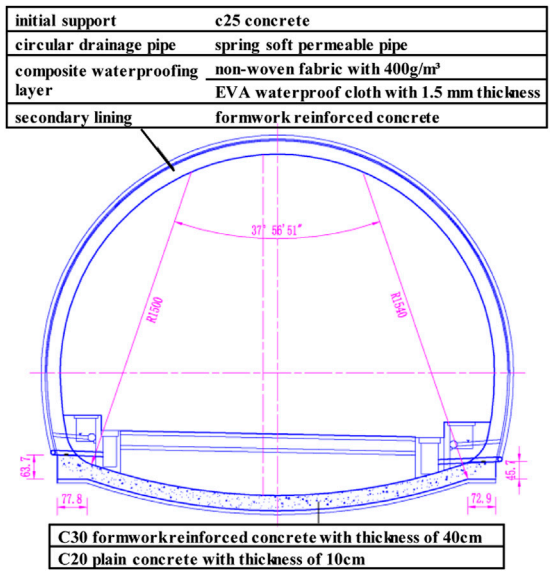

FIGURE 18 | Cross section of the added inverted arch (unit: cm).

(6) There is no inverted arch in the road uplift section, and the problem of excess hydrostatic pressure that cannot be resisted by road weight has not been solved.

REINFORCEMENT MEASURES FOR TUNNEL DISEASES

Analysis of the causes of Nanshibi Tunnel diseases shows that on the one hand, the distribution of karst and water channels revealed by geophysical prospecting is highly consistent with the distribution of tunnel diseases. This proves that karst topography and groundwater are significant causes of the diseases of Nanshibi Tunnel. Therefore, a critical countermeasure for treating tunnel diseases in karst water-rich areas is to accurately and thoroughly block water-diversion channels, strengthen the weak filling medium of the cavity, and directly reduce the water pressure acting on the tunnel lining structure. On the other hand, the secondary lining section with insufficient bearing capacity should be demolished, replaced, or reinforced to ensure that the structure has sufficient safety redundancy to resist the effects of adverse influencing factors. Based on these ideas, a classification treatment and comprehensive disposal scheme of "surrounding rock grouting + lining replacement + adding inverted arch" are proposed.

Grouting of the Surrounding Rock

According to the treatment principle of "segmented governance, highlighting the key points, source plugging, and deep blocking" based on the detection results and the surrounding rock conditions exposed by drilling, a comprehensive grouting treatment was performed for the surrounding rock in the key diseased areas of the tunnel:

(1) Curtain grouting was carried out in sections ZK172 + 460 to ZK172 + 538, ZK172 + 595 to ZK172 + 645, ZK172 + 291 to ZK172 + 309, and YK172 + 610 to YK172 + 660 with karst cave development, rock fragmentation, and water-diversion channel aggregation. A grouting reinforcement circle was formed within 10–20 m of the tunnel excavation contour line to block the arch wall and the vault's water channel completely and to systematically strengthen the weak filling medium of the cavern (shown in **Figures 12**, **13**).

(2) Floor grouting was carried out in the sections ZK172 + 458 to ZK172 + 538, ZK172 + 596 to ZK172 + 644, YK172 + 612 to YK172 + 660, and YK172 + 210 to YK172 + 550 with strong connectivity of surrounding rock fragmentation, karst development, and karst pipelines and fractures in the tunnel floor. A water-repellent reinforcement layer was formed within the range of 10–15 m from the bottom plate. This layer separates the water-conducting channels from the surrounding rocks on both sides of the road surface and systematically strengthens the weak filling medium of the cavern below the bottom plate (shown in **Figures 14**–**16**).

Lining Replacement

The secondary lining of the surrounding rock grouting reinforcement section and insufficient safety factor section was replaced. The replaced lining was a reinforced concrete structure, and an inverted arch was set. The bearing capacity and safety redundancy of the structure were improved to ensure that the safety factor of the structure was not less than the target value. This also helped avoid the direct effect of groundwater on the pavement structure, improved the waterproofing ability of the structure, and reduced the possibility of pavement uplift and cable trench tilt disease as much as possible (shown in **Figure 17**).

Addition of an Inverted Arch

By analyzing the results of the comprehensive geophysical prospecting method along with the range of gushing water and mud and by studying topography and geomorphology and geological prospecting conclusions of the tunnel over the years, inverted arches were added in sections YK172 + 210 to YK172 + 400, YK172 + 480 to YK172 + 564, and YK172 + 660 to YK172 + 70, which are likely to undergo groundwater redistribution and accumulation after the grouting reinforcement of the surrounding rock. The inverted arches were added to improve the structural bearing capacity and reduce the risk of pavement diseases (shown in **Figure 18**).

ANALYSIS OF THE REMEDIATION EFFECT

After completing the treatment of Nanshibi Tunnel, the waterproofing performance of the tunnel was reconstructed, and the safety performance of the lining structure was greatly improved. Tunnel operation was restarted, and the operation was continued through two rainy seasons. During this period, no water leakage or mud burst occurred. Only few wet stains appeared on the surface of the structure, and the statistical analysis reached the secondary waterproof standard of

underground engineering. The lining structure showed no signs of structural diseases such as cracking, breakdown, or pavement uplift; hence, it was safe and stable. The measured lining thickness and strength were verified numerically. Under the combined effect of surrounding rock pressure and hydrostatic pressure, the safety coefficient of the reinforced concrete lining was not less than 3.0, which meets the set target requirements.

The actual operation of the tunnel shows that the countermeasures formulated for the diseases of Nanshibi Tunnel are reasonable and successful and that the tunnel operation is in good condition at present.

CONCLUSION AND RECOMMENDATIONS

(1) Based on the Nanshibi Tunnel project, a refined geophysical exploration scheme was proposed for a complex karst geological structure environment. By combining various geophysical methods (high-density resistivity method, transient electromagnetic method, geological radar method, and seismic imaging method), the full coverage and accurate detection of the karst structure, water passage, and tunnel lining diseases were realized.

(2) Based on the detection results and historical disease data, the causes of the Nanshibi Tunnel diseases were systematically analyzed. The distribution of karst and diversion channels was found to be highly consistent with the tunnel disease distribution. Karst and groundwater are the main causes of lining cracking, water–mud inrush, and inverted arch uplift of the tunnel.

(3) Combined with the existing engineering experience, the concept of the classified and comprehensive treatment of "surrounding rock grouting + lining replacement + adding inverted arch" for tunnel diseases in karst areas was proposed, and it was successfully applied to the supporting engineering methods. Thus, the technical problems of karst tunnel diseases that recur frequently and are difficult to treat completely were systematically solved. The practical experience shows that the key to the treatment of tunnel diseases in karst water-rich areas is to accurately and thoroughly seal the water-diversion channel, strengthen the weak filling medium of the cavity, reduce the water pressure directly acting on the tunnel lining structure, replace or reinforce the lining with insufficient bearing capacity, and ensure that the structure has sufficient safety redundancy to resist the adverse effects.

DATA AVAILABILITY STATEMENT

The original contributions presented in the study are included in the article/Supplementary Material, further inquiries can be directed to the corresponding authors.

AUTHOR CONTRIBUTIONS

ShJ: Writing the review, editing, and methodology. ZH: Writing—original draft, numerical simulation, and analysis. WL: Numerical simulation and in-site monitoring. ZZ and SoJ: Modification. SX: Modification. LZ: Data curation.

REFERENCES

Bangning, K. (2021). Research on the Karst Detection and Collapse Treatment Scheme of High Speed Railway Tunnel. *Railway Eng. J.* 38, 80–84. (in Chinese). doi:10.3969/j.issn.1006-2106.2021.02.015

Ding, W., Gong, C., Mosalam, K. M., and Soga, K. (2017). Development and Application of the Integrated Sealant Test Apparatus for Sealing Gaskets in Tunnel Segmental Joints. *Tunnelling Underground Space Technol.* 63, 54–68. doi:10.1016/j.tust.2016.12.008

Fan, H., Zhang, Y., He, S., Wang, K., Wang, X., and Wang, H. (2018). Hazards and Treatment of Karst Tunneling in Qinling-Daba Mountainous Area: Overview and Lessons Learnt from Yichang-Wanzhou Railway System. *Environ. Earth Sci.* 77, 679. doi:10.1007/s12665-018-7860-1

Gong, C., Ding, W., Mosalam, K. M., Günay, S., and Soga, K. (2017). Comparison of the Structural Behavior of Reinforced concrete and Steel Fiber Reinforced concrete Tunnel Segmental Joints. *Tunnelling Underground Space Technol.* 68, 38–57. doi:10.1016/j.tust.2017.05.010

Gong, C., Ding, W., Soga, K., and Mosalam, K. M. (2019). Failure Mechanism of Joint Waterproofing in Precast Segmental Tunnel Linings. *Tunnelling Underground Space Technol.* 84, 334–352. doi:10.1016/j.tust.2018.11.003

Gongyu, L., and Wanfang, Z. (1999). Sinkholes in Karst Mining Areas in China and Some Methods of Prevention. *Eng. Geology.* 52, 45–50. doi:10.1016/s0013-7952(98)00053-2

He, C., and Wang, B. (2013). Research Progress and Development Trends of Highway Tunnels in China. *J. Mod. Transport.* 21, 209–223. doi:10.1007/s40534-013-0029-4

Huang, F., Zhao, L., Ling, T., and Yang, X. (2017). Rock Mass Collapse Mechanism of Concealed Karst Cave beneath Deep Tunnel. *Int. J. Rock Mech. Mining Sci.* 91, 133–138. doi:10.1016/j.ijrmms.2016.11.017

Huang, L., Ma, J., Lei, M., Liu, L., Lin, Y., and Zhang, Z. (2020). Soil-water Inrush Induced Shield Tunnel Lining Damage and its Stabilization: A Case Study. *Tunnelling Underground Space Technol.* 97, 103290. doi:10.1016/j.tust.2020.103290

Jia, C., Zhang, Q., Lei, M., Zheng, Y., Huang, J., and Wang, L. (2021). Anisotropic Properties of Shale and its Impact on Underground Structures: An Experimental and Numerical Simulation. *Bull. Eng. Geol. Environ.* 80, 7731–7745. doi:10.1007/s10064-021-02428-7

JTG/T D71-2004 (2004). *Design Specification for Traffic Engineering of Highway Tunnel*. Beijing, China: China Communications Press. (in Chinese).

Junfeng, Z., Qiang, L., Yongyue, S., and Lei, W. (2021). On Development Law of Karst Water and Prediction of Water Inflow in a Tunnel in Southest China. *Mod. Tunnelling Technol.* 58, 14–21+50. (in Chinese). doi:10.13807/j.cnki.mtt.2021.02.003

Lei, M., Li, J., Zhao, C., Shi, C., Yang, W., and Deng, E. (2021a). Pseudo-dynamic Analysis of Three-Dimensional Active Earth Pressures in Cohesive Backfills with Cracks. *Soil Dyn. Earthquake Eng.* 150, 106917. doi:10.1016/j.soildyn.2021.106917

Lei, M., Lin, D., Huang, Q., Shi, C., and Huang, L. (2020). Research on the Construction Risk Control Technology of Shield Tunnel underneath an Operational Railway in Sand Pebble Formation: A Case Study. *Eur. J. Environ. Civil Eng.* 24, 1558–1572. doi:10.1080/19648189.2018.1475305

Lei, M., Liu, L., Shi, C., Tan, Y., Lin, Y., and Wang, W. (2021b). A Novel Tunnel-Lining Crack Recognition System Based on Digital Image Technology. *Tunnelling Underground Space Technol.* 108, 103724. doi:10.1016/j.tust.2020.103724

Lei, M., Zhu, B., Gong, C., Ding, W., and Liu, L. (2021c). Sealing Performance of a Precast Tunnel Gasketed Joint under High Hydrostatic Pressures: Site Investigation and Detailed Numerical Modeling. *Tunnelling Underground Space Technol.* 115, 104082. doi:10.1016/j.tust.2021.104082

Liu, C., Lei, M.-f., Peng, L.-m., and Shi, C.-h. (2020). Cavity Influence on Fatigue Performance of Heavy Haul Railway Tunnel's Bottom Structure. *Construction Building Mater.* 251, 118886. doi:10.1016/j.conbuildmat.2020.118886

Min-qing, Z., Hong-jian, H., and Si-ming, T. (2007). Safe Design,Construction and Management of Karst Tunnel. *J. Railway Eng. Soc.* 24, 75–81. 85(in Chinese). doi:10.3969/j.issn.1006-2106.2007.05.016

Richards, J. A. (1998). Inspection, Maintenance and Repair of Tunnels: International Lessons and Practice. *Tunnelling Underground Space Technol.* 13, 369–375. doi:10.1016/S0886-7798(98)00079-0

Tang, Q., Lei, M., Zhu, B., Peng, L., Wu, W., and Shi, C. (2021). Design and Application of Risk Early Warning System for Subway Station Construction Based on Building Information Modeling Real-Time Model. *Advances Civil Engineering* 2021, 1–12. doi:10.1155/2021/8898893

Wang, X., Li, S., Xu, Z., Hu, J., Pan, D., and Xue, Y. (2019). Risk Assessment of Water Inrush in Karst Tunnels Excavation Based on normal Cloud Model. *Bull. Eng. Geol. Environ.* 78, 3783–3798. doi:10.1007/s10064-018-1294-6

Yao, H., Gao, F., Yu, S., and Dang, W. (2017). Construction Risks of Huaying Mount Tunnel and Countermeasures. *Front. Struct. Civ. Eng.* 11, 279–285. doi:10.1007/s11709-017-0414-x

Zhang, R. (2019). Catastrophe Analysis of Deep Tunnel above Water-Filled Caves. *J. Cent. South. Univ.* 26, 1820–1829. doi:10.1007/s11771-019-4136-1

Zhao, C., Lei, M., Shi, C., Cao, H., Yang, W., and Deng, E. (2021). Function Mechanism and Analytical Method of a Double Layer Pre-support System for Tunnel underneath Passing a Large-Scale Underground Pipe Gallery in Water-Rich sandy Strata: A Case Study. *Tunnelling Underground Space Technol.* 115, 104041. doi:10.1016/j.tust.2021.104041

Zhu, J.-q., and Li, T.-z. (2020). Catastrophe Theory-Based Risk Evaluation Model for Water and Mud Inrush and its Application in Karst Tunnels. *J. Cent. South. Univ.* 27, 1587–1598. doi:10.1007/s11771-020-4392-0

Conflict of Interest: Authors SJJ, WL, ZC, SX, and SJ were employed by Shandong Provincial Communications Planning and Design Institute Group Co., Ltd.

The remaining authors declare that the research was conducted in the absence of any commercial or financial relationships that could be construed as a potential conflict of interest.

Publisher's Note: All claims expressed in this article are solely those of the authors and do not necessarily represent those of their affiliated organizations, or those of the publisher, the editors and the reviewers. Any product that may be evaluated in this article, or claim that may be made by its manufacturer, is not guaranteed or endorsed by the publisher.